

A Deep Learning Approach to Probabilistic Forecasting of Weather

NICK RITTLER , CARLO GRAZIANI , JIALI WANG, RAO KOTAMARTHI

Argonne National Laboratory

ABSTRACT: We discuss an approach to probabilistic forecasting based on two chained machine-learning steps: a *dimensional reduction* step that learns a reduction map of predictor information to a low-dimensional space in a manner designed to preserve information about forecast quantities; and a *density estimation* step that uses the probabilistic machine learning technique of normalizing flows to compute the joint probability density of reduced predictors and forecast quantities. This joint density is then renormalized to produce the conditional forecast distribution. In this method, probabilistic calibration testing plays the role of a regularization procedure, preventing overfitting in the second step, while effective dimensional reduction from the first step is the source of forecast sharpness. We verify the method using a 22-year 1-hour cadence time series of Weather Research and Forecasting (WRF) simulation data of surface wind on a grid.

1. Introduction

Weather forecast capabilities are crucial to energy market operations, regulation, and policymaking, as well as infrastructure maintenance and planning. Probabilistic forecasting of weather in particular (Palmer 2002; Zhu et al. 2002; Gneiting et al. 2008) is widely accepted and preferred in practice, largely due to the fact that a probabilistic forecast, i.e. a *distribution* over future outcomes, captures the uncertainty of the situation in a way that simple “point” predictions fail to do. However, limitations in physics and the need for higher spatial resolutions have limited the use of probabilistic forecasting for variables such as surface temperature, wind speeds and other weather variables of interest (Hirschberg et al. 2011). Thus, probabilistic forecasting still presents an important, and challenging problem.

The growing interest in machine learning in the past decade has resulted in a corresponding growth in machine learning-based weather forecasting literature. We observe, however, that modeling weather events in this literature has often focused on the reduction of forecasting tasks to classification or point prediction settings, be it through fully data-driven techniques, or via the application of machine learning techniques as a post-processing step following physics-based modeling. Papers in the former category include Jergensen et al. (2020), Sprenger et al. (2017), Fabian et al. (2007), and Roebber et al. (2007); papers in the later category include Yuan et al. (2007), Burke et al. (2020), and Schaumann et al. (2021).

Interestingly, this focus is somewhat in contrast with the probabilistic forecasting community at large, wherein there has been significant work on the application of machine learning to produce probabilistic forecasts (Shi and Yeung 2018; Lim and Stephen 2021). One of most common

general approaches in this literature is the statistical learning of complex functions taking in current information and outputting parameters governing a distribution over future outcomes; the modeling of these functions has been done by methods that include recurrent neural networks (Salinas et al. 2020), convolutional neural networks (Chen et al. 2020), and standard fully connected nets (Vossen et al. 2018).

Research on machine learning of probabilistic forecasts for weather is now beginning to appear. Petersik and Dijkstra (2020), use deep neural networks to learn a non-linear transformation of the current weather conditions into the parameters of a Gaussian mixture to model the El Niño–Southern Oscillation. Grover et al. (2015) produce point predictions of weather conditions at specific locales using standard procedures, use kernel methods to enforce a smooth interpolation between locales, and take a Bayesian approach to produce estimates for the joint posterior distribution of weather conditions across locales.

Our approach to the probabilistic weather forecasting problem is to first learn an explicit dimension reduction, and thus a low dimensional representation of a large spatio-temporal grid of weather measurements, something that is conceptually not all that different from the learning of a transformation of input into distributional parameters. However, instead of enforcing a parametric assumption in the modeling of a future weather event, we non-parametrically learn the distributional relationship of our low dimensional representation with the future outcomes. Until the last few years, procedures in the ML weather forecasting literature have largely relied on rather subjective selection of forecasting predictors from available data, often ignoring the potential that spatio-temporal grids of observations and other high dimensional data sets have for improving forecast quality; though there have been recent efforts to create models with higher dimensional inputs

Corresponding author: Nick Rittler, nrittler@ucsd.edu

(Qui et al. 2017; Mehrkanoon 2019), and though there are notable early exceptions (Nandar 2009), we believe our emphasis on the learning of a low dimensional representation of high dimensional weather data to be both an effective method and a useful illustration of the use of high dimensional data. Given the growth in simulation and observational data sample sizes, the joint modeling of low dimensional representations of the past and possible future observations through non-parametric methods is a promising approach to empirical forecasting with such datasets.

2. Overview of the Methodology

A probabilistic forecast (Gneiting and Katzfuss 2014) over a continuous random variable of interest Y given observations governed by random variables X is a conditional distribution $P(Y|X)$ with density $p(y|x)$, that is, a mapping from a predictor x bearing information about Y to a distribution over possible outcomes of Y . It is well-understood that the essence of the probabilistic forecast is to provide the ability to fully describe the uncertainties in predicted outcomes.

In the case of probabilistic forecasts of weather, x can be made up of weather conditions at various spatio-temporal locations, such as might be provided by readings from an array of weather stations. Alternatively, x might comprise output data from an ensemble of numerical weather prediction (NWP) simulations, which in turn are functions of weather observations through data assimilation procedures. The first case corresponds to what are termed “empirical” forecasts (Van den Dool et al. 2007), whereas the latter case corresponds to “physics-based forecasts” (Toth and Buizza 2019). Our purpose in this work is to focus on the information-theoretic aspects of machine learning-mediated forecasts, and how information embedded in predictors concerning predicted quantities may be maximized. From this perspective, the distinction between the two types of predictors is largely immaterial.

It is useful to introduce the idea of the unique *ideal forecast distribution* (Gneiting and Ranjan 2013; Gneiting and Katzfuss 2014; Graziani et al. 2021) with density $p(y|x)$, which makes maximal use of the information in x . It is intuitively straightforward to see that such a unique distribution exists, as it would be empirically ascertainable in principle by first estimating the joint density $p(x, y)$ by histogramming a large dataset of pairs $\{(x_l, y_l) : l = 1, \dots, N\}$ ($N \gg 1$), and conditioning to estimate $p(y|x)$. A true first-principles ideal forecast distribution for weather is essentially unobtainable, since it would require modeling precision and computational power far beyond what is currently available (Fritsch and Carbone 2004; Knutti and Sedláček

2013). However as the thought experiment indicates, data-driven approximations to ideal forecast distributions may be obtained given sufficient data.

Unfortunately, it is usually the case that the data x is unmanageably large, consisting not only of many samples (which is desirable) but of very large vectors (which is less so). To make progress, x must be processed by a transformation $T(x)$ that effects a dimensional reduction. Clearly, $T(x)$ must be chosen with a view to limiting damage to the information that x bears with respect to y . As we will see below, it is often quite practical to achieve this, because there is frequently much more data mass in x than is strictly necessary to code information concerning y . Making judgments concerning the appropriate choice of reductions $T(\cdot)$ requires comparing the properties of the distributions $P(Y|X)$ and $P(Y|T(X))$, as we will discuss below.

Another concept that we make essential use of below is that of probabilistic calibration (Gneiting and Ranjan 2013; Gneiting and Katzfuss 2014). Probabilistic calibration is a desirable feature in a forecast because it means that the forecast is “honest” about the probabilities of its quantiles, since those probabilities correspond to long-term average frequencies that are expected in a forecast system based on the reduction $T(\cdot)$ that furnishes an approximation to the ideal forecast distribution $P(Y|T(X))$.

As mentioned above, we approach the probabilistic forecasting task in two main steps. The first is learning of a suitable $T(\cdot)$ that reduces the dimension of predictors x while retaining as much information about the response as possible. The second is joint modeling of the distribution of the artificial predictors $T(x)$ and the response. Once the joint modeling is complete, a numerical integration of the modeled density yields the forecast, i.e. the density $q(y|T(x))$ corresponding to the distribution $P(Y|T(X))$.

Reduction of dimension via $T(\cdot)$ is necessary, because the number of data samples required to model a joint density essentially increases exponentially in the number of dimensions to be considered. Despite this, the goal is to make forecasts as precise as possible, while still retaining calibration. This is the principle of “maximizing sharpness subject to calibration” (Gneiting et al. 2007). Thus, a major part of this work is the efficacy of the dimension reduction technique.

In our experience with our two-step forecasting procedure, the problem of maximizing sharpness subject to calibration has turned out to separate into two essentially independent problems. In the first step, we maximize forecast “sharpness” — a measure of concentration of the forecast distribution to small outcome sets (Gneiting et al. 2007) — by minimizing the Kullback-Leibler divergence between $P(Y|X)$ and $P(Y|T(X))$, which turns out to be equivalent to maximizing the mutual information between Y and $T(X)$

with respect to the choice of $T()$. This is described in §4. We verify the increased sharpness of our computed forecasts relative to that produced using plausible alternative dimensional reductions using entropy games (Graziani et al. 2021), a recasting of “ignorance scoring” (Roulston and Smith 2002), as described in §5.

Calibration then comes down to properly modeling the joint distribution of the low dimensional representations $T(X)$ and the responses Y . We test calibration by observing what percentage of test set examples fall in modeled probability contours in our forecasts. Specifically, for each predictor in the test set, we can forecast the response using our models. Each forecast is a density of response, and so we can compute probability contours for this density. Over the entire test set, we can see what percentage of true test responses fall within the modeled .683 and .954 contours. Of course, if the forecasts are in line with the data generating distribution, then up to noise in sampling the test set from the data generating distribution and rounding errors, we should see .683 and .954 of the test samples fall within the respective modeled contours. Though this is obviously not a sufficient condition for calibration, it is a useful necessary condition that gives rough idea of how honestly our forecasts deal with uncertainty. This procedure is described in greater detail in §5.

3. Description of the Data, their Handling

In this section, we describe the datasets used to verify our machine learning methodology. This description of the data is useful to have in advance of the detailed methodological development, since it can help clarify and motivate the technical aspects of our work.

The data are zonal and meridional winds that are the output of historical simulations based on a widely used mesoscale weather model, Weather and Research Forecasting (WRF) model; the simulations were run between the years 1980-2010 at a grid resolution of 12 km x 12km and with output saved once every 3 hours (Wang and Kotamarthi 2014). We consider in particular a 19x19 box of spatial locations around Kansas City at highest resolution afforded by the simulation, between the years 1984 and 2005. We specify the task of forecasting these two components of wind at $t + 3$ hours at the center of our grid, using all wind data from around the grid at times $t, \dots, t - k$. The 3 hour forecasting window is specified so that measurements from such a relatively small box of values are informative of the response; forecasting weather further into the future would require a larger grid of observations.

We formulate examples (y_i, x_i) by letting y_i be the 2-dimensional wind vector at the center of the grid at timestep $i + 1$, and letting x_i be the concatenation of wind vectors around the grid at time steps $i, \dots, i - k$, for some positive

integer k . Given the small size of the box and the characteristic time- and length scales of the wind patterns, not much information about the response is contained when $k > 3$, so we settle on $k = 3$.

For any given model that we train, we restrain the model to consider small “seasonal” slices of three months of each year. Thus, a typical model is trained using some number of years of “winter” examples, and likewise validated on winter examples; by “winter” we specifically mean the 3 months of year’s worth of 3-hour timesteps, by “spring”, the second three months, etc. We treat (y_i, x_i) as though they are drawn independently and identically distributed from some distribution \mathcal{D} ; the restriction to seasonal slices simplifies the process of approximating \mathcal{D} significantly. Secular drift of the weather is a concern, but in training we avoided this issue by ignoring the temporal positions of the samples.

Our training, validation, and testing procedures are as follows. We first separate a test set of the observations from the most recent seasonal slice, e.g. the “winter” from the most recent year in a specified range of years. We then take winter observations from the previous 10 years, and divide these examples uniformly at random into dimension reduction training, joint model training, and validation sets. The validation set is used for model selection in both the dimension reduction and joint modeling. The test set is not consulted until after all final modeling decisions have been made. We observe the test set to measure forecast precision and confirm calibration of our forecasts on true holdout data, and in particular, holdout data from a never before seen season in the “future”. Here secular drift of the weather does come into play, and so confirmation of calibration on these future weather samples is vital.

4. Dimension Reduction

Dimension reduction of the predictors is a necessary step in any continuous probabilistic forecasting scheme based on a dataset with high dimensional features, since density estimation in high-dimensional spaces is well-known to be challenging (Silverman 2018). Naturally, this is often the case for geoscientific data, where large spatial and temporal variabilities abound. To understand the most important patterns (including time and space) of a dataset, one needs to use dimensional reduction technique to reduce the data to certain dimension, from which one can understand the importance of each pattern (in space) and how that pattern change with time. However, fully unsupervised dimension reduction techniques such as Principal Component Analysis (PCA) are inadequate for the purposes of forecasting, as they only project predictors onto informative subspaces, ignoring the relationship of predictors and response. With this in mind, we employ a dimension reduction technique

that is focused on preserving as much information about the response as possible.

a. Information Preserving Reductions

Information theory furnishes a useful framework in which to explore these ideas formally, and is at the basis of the method we use. Indeed, there is a well-developed literature of dimension reduction for supervised learning that follows the same ideas as we use here; see for example (Leiva-Murillo and Antonio 2007) and (Shadvar 2012).

We briefly review the required information-theory background (see Cover and Thomas 1991, for a detailed treatment). Given a pair of random variables (Y, X) with a joint distribution $P(X, Y)$ assumed absolutely continuous for simplicity, and hence possessed of a density $p(x, y)$; and given marginal distributions $P(X), P(Y)$ with densities $p_x(x), p_y(y)$, the mutual information $I(Y; X)$ is defined by

$$I(Y; X) = KL [p(x, y) || p_x(x)p_y(y)], \quad (1)$$

where KL denotes the Kullback-Leibler divergence, given by the formula

$$KL [p(z) || q(z)] \equiv \int dz p(z) \log \left[\frac{p(z)}{q(z)} \right]. \quad (2)$$

The Kullback-Leibler divergence (Kullback and Leibler 1951) is a measure of the difference of two distributions. It has the property of being bounded below by zero, a value attained when the densities $p(z)$ and $q(z)$ are equal almost everywhere. It follows from this the mutual information $I(Y; X)$ is small when $p(x, y)$ can approximately be factored into marginals, i.e. when X hardly any information about Y .

Now consider a dimensional reduction $T : \mathbb{R}^d \rightarrow \mathbb{R}^m$, $m < d$. The forecast distribution conditioned on X is $P(Y|X)$. As we discussed in §2, this distribution is in principle (if perhaps not in practice) empirically ascertainable by histogramming a large database of pairs (y, x) . On the other hand, after reduction by $T(\cdot)$, we are concerned with the forecast distribution $P(Y|T(X))$. This distribution is in principle “degraded” by information loss with respect to $P(Y|X)$. The KL divergence and the mutual information are tools that allow us to choose $T(\cdot)$ such that these two distributions are as close as possible given m , up to sampling and optimization considerations.

The reduction $T(\cdot)$ implicitly defines a new random variable $\hat{T} \equiv T(X)$. We proceed by considering the KL divergence of $P(Y|X)$ and $P(Y|\hat{T})$,

$$\begin{aligned} K(X) &\equiv KL [P(Y|X) || P(Y|\hat{T})] \\ &= \int dy p(y|X) \log \left[\frac{p(y|X)}{q(y|T(X))} \right]. \end{aligned} \quad (3)$$

Since we have a sample of realizations from the random variable X from which to estimate this quantity, we average Equation (3) by taking the expectation under $P(X)$ using the corresponding density $p(x)$:

$$\begin{aligned} \mathcal{E}_{X \sim P(X)} \{K(X)\} &= \int dx dy p(x) p(y|x) \\ &\quad \times \log \left[\frac{p(y|x)}{q(y|T(x))} \right] \\ &= \int dx dy p(x, y) \\ &\quad \times \log \left[\frac{p(x, y) q(T(x))}{p(x) q(T(x), y)} \right]. \end{aligned} \quad (4)$$

In Equation (4) we have introduced new densities $q(t)$ and $q(t, y)$ corresponding to the distributions $P(\hat{T}), P(\hat{T}, Y)$, where t is a realization of \hat{T} . We may now insert a factor of $p(y)$ into the numerator and denominator of the log term in Equation (4), and split the log term, to obtain

$$\mathcal{E}_{X \sim P(X)} \{K(X)\} = I(Y; X) - I(Y; \hat{T}). \quad (5)$$

In Equation (5), only the second term depends on the choice of the reduction function $T(\cdot)$. We can therefore see that choosing a reduction that minimizes the average information divergence between $P(Y|X)$ and $P(Y|\hat{T})$ is equivalent to choosing $T(\cdot)$ to maximize the mutual information between Y and $\hat{T} = T(X)$.

The approach we take it is train a neural network $T : \mathbb{R}^d \rightarrow \mathbb{R}^m$ from a shallow but flexible class of networks by maximizing an empirical estimate of the expected mutual information between Y and $T(X)$ with respect to the parameters defining the network. In the next subsection we describe practical implementations of this approach.

b. Computing and Maximizing the Objective

In principle, the goal of optimizing the dimensional reduction $T(\cdot)$ can be attained by choosing as maximization objective an empirical estimate for the average KL-divergence:

$$\max_{T \in \Theta} \frac{1}{N} \sum_{i=1}^N \log \left(\frac{q(y_i, T(x_i))}{q(T(x_i))} \right), \quad (6)$$

where Θ denotes the set of all functions that can be represented by whatever neural network architecture chosen. There is a difficulty, however, in that estimates of the densities $q(y, t)$ and $q(t)$ must be produced at each iteration, because the densities depend on the transformation $T(\cdot)$,

and so evolve as $T(\cdot)$ evolves. This circumstance compounds the computational challenge already inherent in empirical density estimation.

We experimented with k -nearest neighbors density estimation. Essentially, once k has been specified, the density estimate for any given point $(y_i, T(x_i))$ is

$$\hat{\pi}(y_i, T(x_i)) = \frac{k}{N} \frac{1}{\text{Vol}_k(y_i, T(x_i))},$$

where $\text{Vol}_k(y_i, T(x_i))$ is the volume of the k^{th} smallest parallelepiped in the set of $p+m$ dimensional parallelepipeds defined by $(y_i, T(x_i))$ and the other points in the training set. In order to get good density estimates, large minibatches are required in the optimization, which slows down convergence to an unacceptable degree. In the end, we opted to abandon this approach due to fragility and poor performance.

Another option for estimating the densities in Equation (6) would be to resort to the probabilistic machine learning technique of normalizing flows that we describe in §5 below, which we use to estimate the forecast density. This would have the effect of inserting a second expensive ML training loop in our workflow, and probably turning the problem into a true high-performance computing (HPC) enterprise. This approach is worth considering in the future, but for simplicity in this work we adopted a normal-theory approximation that we now describe.

The objective is radically simplified if we simply approximate the joint distribution of (Y, \hat{T}) as Gaussian. Suppose this assumed normal distribution is governed by a covariance given in block form by

$$\Sigma \equiv \begin{bmatrix} \Sigma_{YY} & \Sigma_{Y\hat{T}} \\ \Sigma_{\hat{T}Y} & \Sigma_{\hat{T}\hat{T}} \end{bmatrix} \quad (7)$$

Then using standard normal theory arguments one can show that the mutual information $I(Y; \hat{T})$ is given by the expression

$$I(Y; \hat{T}) = -\frac{1}{2} \ln \left[\det \left(\Sigma_{YY} - \Sigma_{Y\hat{T}} \Sigma_{\hat{T}\hat{T}}^{-1} \Sigma_{\hat{T}Y} \right) \right] + \frac{1}{2} \ln [\det \Sigma_{YY}]. \quad (8)$$

Thus in this approximation, minimization of the expected KL divergence in Equation (5), which is equivalent to maximization of $I(Y; \hat{T})$, is in turn equivalent to

$$\min_{T \in \Theta} \ln \left[\det \left(\Sigma_{YY} - \Sigma_{Y\hat{T}} \Sigma_{\hat{T}\hat{T}}^{-1} \Sigma_{\hat{T}Y} \right) \right], \quad (9)$$

that is, to minimizing the predictive variance of $y|T(x)$.

We implement this approximation by computing empirical data covariances from the data to obtain the elements of the array in Expression (7). We have found the resulting data reduction procedure to be far more rapid and robust than any based on density estimation, despite the occasionally questionable nature of the Gaussian assumption for data that clearly exhibits non-Gaussian features.

c. Target Dimensions and Sufficient Dimension Reduction

It is a known result of normal theory that given that a response y of dimension p and predictors x of dimension d that have a jointly normal distribution in $p+d$ dimensions, there exists an affine transformation $T: \mathbb{R}^d \rightarrow \mathbb{R}^p$ that is fully information preserving. More precisely, there exists an affine $T: \mathbb{R}^d \rightarrow \mathbb{R}^p$ such that

$$\forall x, KL[n_x(y|x) || n_T(y|T(x))] = 0, \quad (10)$$

where $n_x(y|x)$ is the normal predictive density of y conditioned on x , and $n_T(y|T(x))$ is the normal predictive density of y conditioned on $T(x)$.

This result has an intuitively reasonable explanation: a normal distribution is specified by its mean and variance alone, and since the conditional variance of $y|x$ is independent of x , then given the joint covariance structure of (y, x) , the family of distributions $y|x$ is entirely specified by the conditional mean, which is a p -dimensional linear function of x . The conditional mean is in fact the dimensional reduction $T(x)$ in this case. In the statistics literature, the idea of the distribution of the response conditional on the predictors being invariant to a specific transformation of the predictors into some lower dimensional space is known as ‘‘sufficient dimension reduction,’’ (Adraghi and Cook 2009).

The relevance for our task is that that the reduced dimension m should be expected to be commensurate — if not precisely equal, as in the normal theory case — to the output dimension p , so that when the output dimension is much smaller than the input dimension of the predictors, radical dimensional reductions are in principle possible. In the case of our simulated wind data, where we predict the two wind components at one grid point, we would expect a very considerably reduced dimensionality ($m = 2$, in fact) in the normal case. For many applications where data are approximately jointly normal, there’s no reason to believe that $m \gg p$ reduced predictors are required to capture the majority of the information stored in the d dimensional raw predictors.¹

¹Note that the reductions that we consider here are only information-preserving with respect to the chosen forecast quantities, and not preserving of general information. They are in general expected to be very information-lossy with respect to other predicted quantities.

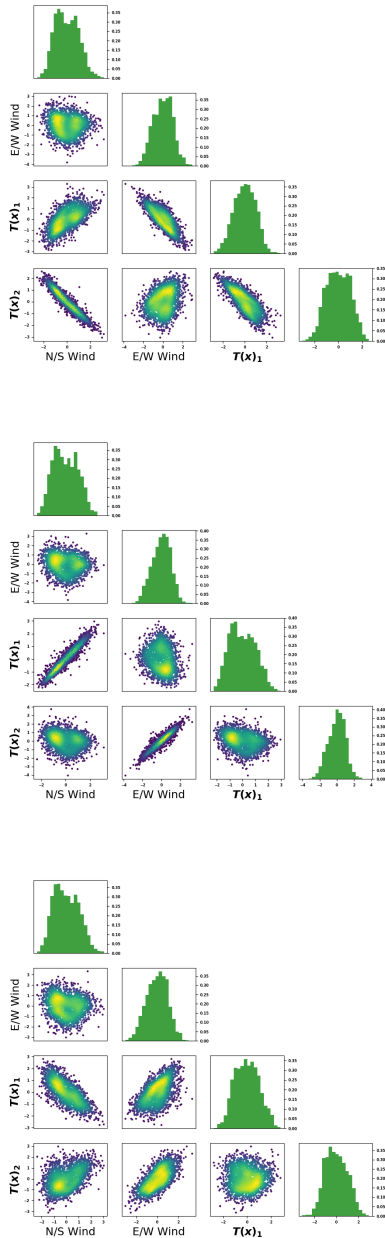


FIG. 1. Plots of the training data resulting from the three dimension reduction techniques used in the experiments on the Jan-March seasonal slice, with Year 1 response. On the top, the result of the information preserving reduction with normal approximation, in the middle, grid point choosing, and finally PCA at the bottom. $T(x)_1$ and $T(x)_2$ denote the artificial predictors; the map T is learned in dimension reduction.

In practice, we have indeed set m to be p in our numerical experiments. Of course, higher dimensional m could and should be explored, depending on the size of the dataset at hand. For large data sets, it is possible that

the extra dimensions for artificial predictors are helpful in sharpening forecasts at moderate extra cost, but this may not be the case for smaller datasets, where a lack of training examples in a higher dimensional regime may make calibration of the forecasts hard or impossible.

Despite the fact that our data are by no means jointly normal this normal approximation has proved to be effective in producing sharp forecasts and lower training times. There is some approximate normality in the raw predictors, which may be part of the reason we have found small m sufficiently information preserving.

5. Producing Probabilistic Forecasts

Given a dimension reducing transformation $T(\cdot)$, the forecasting task next demands a joint modeling of the response y_i and the artificial predictors $T(x_i)$. Given an estimate for the joint distribution of response and predictors, forecasts can be produced by standard numerical integration techniques, as probabilistic forecasts are simply conditional distributions.

a. Normalizing Flows

We model the joint distribution by a neural network-based non-parametric density estimation technique referred to in the literature as the “normalizing flow” (Kobyzev et al. 2019). We briefly review normalizing flows here, consigning more detail to Appendix A1

Given a random variable W taking values in \mathbb{R}^{p+m} with density function p_W , recall that the formula for the density of the random variable V formed by mapping V through the differentiable bijection $\phi : \mathbb{R}^{p+m} \rightarrow \mathbb{R}^{p+m}$; $W = \phi(V)$ is

$$p_V(v) = p_W(\phi(v)) \cdot |\partial\phi|, \quad (11)$$

where $\partial\phi$ denotes the Jacobian matrix of the transformation.

The idea of normalizing flows is thus to fix some W as the “latent” random variable with a known simple distribution density (often a standard normal density or a normal mixture), and given samples of some random variable V taking values in \mathbb{R}^{p+m} , and with unknown density $p_V(v)$, model p_V by learning a differentiable bijection ϕ that satisfies Equation (11). Assume that the latent distribution p_W can be parameterized by $\omega \in \Omega$. We express ϕ as a neural network in some flexible class of functions parameterizable as neural nets Φ , and then simply learn ϕ by maximizing the log-likelihood of the data in the latent space, i.e. we consider the optimization objective

$$\max_{\phi \in \Phi, \omega \in \Omega} \frac{1}{N} \sum_{i=1}^N \log \left(p_W(\phi(v_i); \omega) \right) + \log \left(|\partial\phi(v_i)| \right),$$

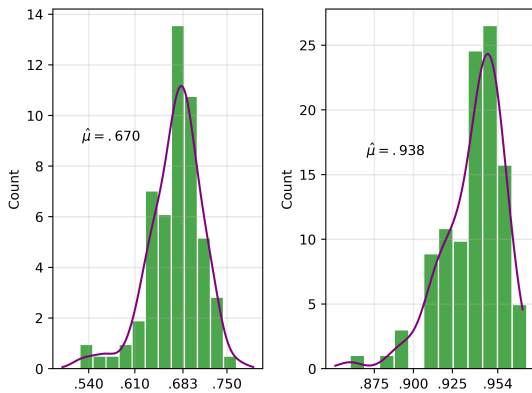


FIG. 2. A histogram constructed from the test set hit rates generated on each year/season combination. The fact that these histograms are approximately centered at .683 and .954 without too much variance is strong evidence that our forecasts are indeed calibrated. We do see that the average hit rates are in both cases a bit too small, meaning that our forecasts tend to be slightly “too certain” about the future.

and use a gradient-descent approach simultaneously on ω , and the parameters characterizing ϕ .

b. Training Joint Distributions for Calibration

One of the canonical issues in machine learning practice is overfitting (Goodfellow et al. 2016). In a nutshell, overfitting is the phenomenon of an extremely expressive model beginning to model “features” in the training data that are due to sampling noise, rather than to the generating distribution. The result is well-understood to be a degradation in the generalization capacity of the model. In the context of forecasting, this is tantamount to loss of forecasting skill.

Regularization is the general term for any strategy that combats overfitting. One type of regularization is achieved by monitoring performance on a validation set, and picking the model that performs best on this validation set. To train for calibration, we retain this philosophy, although perhaps not in the most standard way.

Instead of picking the model with best validation loss, we employ an early stopping strategy centered around achieving calibration on the validation set. For a probabilistic forecast to be useful at all it is necessary that it be probabilistically well-calibrated, and we therefore design our regularization strategy around calibration. We train the model for some relatively large number of iterations, well beyond the point where the training loss is no longer obviously improving; we stuck to 1200 steps of gradient descent for our simulated wind data experiments, but learning rates, etc will play an important role in how many iterations this

takes. Every 100 training steps after some initial learning phase where our joint model is clearly still experiencing drastic improvement on the training set, we consider the current learned model, and do a numerical integration to produce a forecasting machine. With this interim forecasting machine, we can check calibration on the validation set, and in the end, we chose as our final forecasting machine the interim model that was best calibrated on the validation set.

The notion of “best calibrated” was somewhat arbitrarily chosen. As mentioned above, each time we check calibration, we compute the percentage of validation responses falling within the modeled .683 contour, and .964 contour. To compute a calibration score s_c for a given model, we calculate the absolute deviations from nominal contour calibration, and we use the following convex combination of those deviations:

$$s_c := \frac{13}{23} |.683 - hr_{.683}| + \frac{10}{23} |.954 - hr_{.954}|,$$

where hr_p is the computed percentage of validation examples falling in the model contours, what we often refer to as the “hit-rate” of the p contour. The slight weighting towards the inner contour reflects the observation that often inner contours were more difficult to model in our particular case, as much of the joint distribution detail tends to happen near modes. From a larger methodological perspective, this should simply be viewed as another hyperparameter.

6. Experiments

Our numerical experiments to validate the forecasting software were conducted using the simulated wind data described in §3.

A given experiment is carried out as follows. We fix a recent year in the range 1995 to 2003, and a season in that year. The year and season choice specify the test set, and the training and validation sets are then constructed by taking the examples appearing in the 10 previous examples of the chosen season. We then produce forecasts, and report performance on the test set. The use of 10 previous years is arbitrary; in practice, this figure should be treated as a hyperparameter governing the degree to which the model is informed by recent events.

Performance is measured in two ways. Firstly, we test the models for calibration by computing the “hit rates” for the .683 and .954 contours on test data, just as was done in evaluating calibration of interim models on the validation data during training. We do this for each experiment’s test set, yielding a set of hit rate scores on hold out data. We give histograms of these empirical measure of calibration

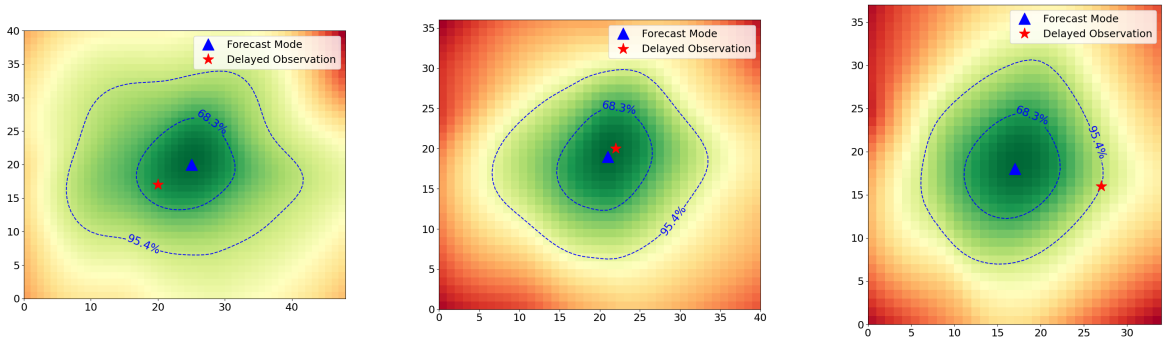


FIG. 3. Visualizations of example forecasts, providing an impression of the hit rate computations. Hit rate computations are performed by computing what percentage of delayed observations fall in the modeled contours.

over this set of scores in Figure 2, giving evidence of approximate calibration via our methods. This is vital, as if forecasts are not properly calibrated, they can be unrealistically certain about the events they forecast, and essentially cheat in competitions of forecast precision, whereby sharper forecasts are preferred, but only conditional on calibration.

After guaranteeing that calibration has been approximately achieved, we can begin to consider precision, or “sharpness”, of forecasts. Assuming proper joint modeling of response and predictors, the sharpness of the forecasts is a direct result of the efficacy of the dimension reduction; it tells us how much information about the response is being “saved” in our low dimensional representation. As such, we use this section to display the advantages of our dimension reduction technique, even with the crude approximation of joint normality in lower dimensions.

As mentioned above, one might naively consider picking m locales that are highly correlated with the response as a form of crude dimension reduction. This is actually a relatively reasonable approach, as some variables at some points on the grid have correlation $>.95$ with corresponding response variables 3 hours in the future. Another dimensional reduction technique that is familiar to machine learning practitioners is PCA. There is no reason to think that PCA is likely to furnish informative data reductions in the current setting, as we are concerned with safeguarding predictor information concerning responses about relationships between response and predictor, and PCA is an unsupervised algorithm that when applied to predictors is agnostic about responses. Nonetheless we include it, given its popularity, as a sort of baseline reduction.

To test sharpness, we play an information theoretic game called the Entropy Game (Graziani et al. 2021), a re-elaboration of the Ignorance Score (Roulston and Smith 2002), between forecasts. This amounts to evaluating the

log-likelihood of the conditional distribution corresponding to each forecast for each instance in the test set at the observed value, and computing the difference in the sums of these log-likelihoods over the test set. Basically, a forecast does well in the entropy game if the evaluated log-likelihoods are usually large at the wind values that were actually observed, which given that probability density functions are normalized, is a reasonable measure of how sharp the forecasts are. As discussed in Roulston and Smith (2002) and Graziani et al. (2021), a forecast that exhibits superior sharpness in this sense can furnish the basis for winning wagers on forecast outcomes against less sharp forecasts, and hence is in a realizable sense a basis for superior decision-making.

Figure 4 shows the sharpnesses of forecasts reduced by the three methods. It is evident from the figure that the normal theory-based dimension reduction has improved sharpness over naive grid point picking, wherein the most correlated locales with future observations are used as predictors; this baseline outperforms PCA, as expected.

7. Discussion

The fact that calibration can approximately be achieved is not necessarily obvious *a priori*. After all, in making up the test set with future observations, we are directly subjecting ourselves to confounding effects of secular weather drift. That being said, calibration on the test set is really a statement about the invariance of the modeled conditional distributions, and it seems clear that these conditional distributions should be much less affected by secular drift than the marginals over the predictors we condition on, i.e. the climatetology. This seems to be a key to the viability of this proposed procedure.

A potential drawback to our approach is the fact that we did not settle on the final experimental design until

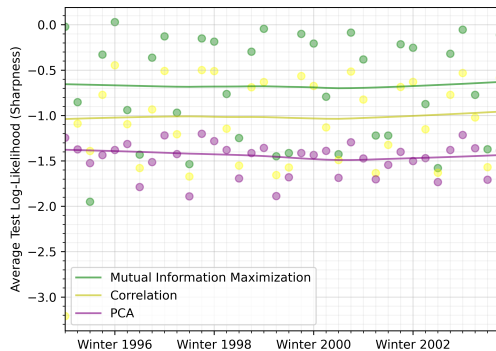


Fig. 4. A visualization of the test likelihoods for each of the three dimension reduction techniques employed, for each of the year/season experiments run. It is very clear that the performance of the information theoretic based dimension reduction technique is an improvement over more naive methods.

after some exploratory experimentation with our models on the data set. It is therefore possible that we implicitly learned something about the hyperparameter settings of our models while analyzing different training-test set splits. We intuitively expect (but have not explicitly shown) that out-of-sample generalization failures due to such model dependencies are weak compared to well-known failures due to in-sample parameter overfitting.

In fact, it is very possible that better results are achievable. In the experiments reported here, we did not exhaustively search hyperparameter space in even in the most important dimensions. For example, the frequency of validation set calibration checks, the weighting towards inner contour validation estimates, the number of dimensions we reduce to, the search over novel architectures in the learning of dimension reductions, and the number of previous seasons to add into the training/validation set are all candidates for investigations that could improve performance. As mentioned above, the choice of updating the model seasonally is arbitrary. It’s quite possible that more frequent updating could improve performance.

As noted in §4, it would be possible to improve on normal theory reduction by incorporating a second normalizing flow training loop at the dimensional reduction stage, so as to obtain estimates of the probability densities in the expression for objective function of Equation (6). This training would have to be repeated at every step of the gradient descent over the parameters of the reduction function $T(\cdot)$. This would in principle make the computation a truly HPC-scale problem, although it is possible to imagine ways of abating the cost by making the two optimizations — over $T(\cdot)$ and over NF parameters — aware of each other. The benefit of such an approach would depend on the degree to which the non-Gaussian nature of

the data limits the information-preservation properties of the normal theory approximation.

8. Acknowledgements

This material is based upon work supported by Laboratory Directed Research and Development (LDRD) funding from Argonne National Laboratory, provided by the Director, Office of Science, of the U.S. Department of Energy under Contract No. DEAC02-06CH11357.

9. Data Availability Statement

All data and code used in this work are publicly accessible via the following repository: https://github.com/rittlern/probabilistic_forecasting.

10. Government License

The submitted manuscript has been created by UChicago Argonne, LLC, Operator of Argonne National Laboratory (“Argonne”). Argonne, a U.S. Department of Energy Office of Science laboratory, is operated under Contract No. DE-AC02-06CH11357. The U.S. Government retains for itself, and others acting on its behalf, a paid-up nonexclusive, irrevocable worldwide license in said article to reproduce, prepare derivative works, distribute copies to the public, and perform publicly and display publicly, by or on behalf of the Government. The Department of Energy will provide public access to these results of federally sponsored research in accordance with the DOE Public Access Plan <https://www.energy.gov/downloads/doe-public-access-plan>.

References

- Adragni, K. P., and D. Cook, 2009: Sufficient dimension reduction and prediction in regression. *Philosophical Transactions of The Royal Society A Mathematical Physical and Engineering Sciences*.
- Burke, A., N. Snook, D. J. Gagne II, S. McCorkle, and A. McGovern, 2020: Calibration of machine learning-based probabilistic hail predictions for operational forecasting. *Weather and Forecasting*.
- Chen, Y., Y. Kang, Y. Chen, and Z. Wang, 2020: Probabilistic forecasting with temporal convolutional neural network. *Neurocomputing*.
- Cover, T., and J. A. Thomas, 1991: *Elements of Information Theory*. John Wiley and Sons.
- Fabian, D., R. de Dear, and S. Lelleyett, 2007: Application of artificial neural network forecasts to predict fog at canberra international airport. *Weather and Forecasting*.
- Fritsch, J. M., and R. Carbone, 2004: Improving quantitative precipitation forecasts in the warm season: A uswrp research and development strategy. *Bulletin of the American Meteorological Society*, **85** (7), 955–965.

- Gneiting, T., F. Balabdaoui, and A. E. Raftery, 2007: Probabilistic forecasts, calibration and sharpness. *Journal of the Royal Statistical Society: Series B (Statistical Methodology)*, **69** (2), 243–268.
- Gneiting, T., and M. Katzfuss, 2014: Probabilistic forecasting. *Annual Review of Statistics and Its Application*, **1** (1), 125–151, <https://doi.org/10.1146/annurev-statistics-062713-085831>, URL <https://doi.org/10.1146/annurev-statistics-062713-085831>, <https://doi.org/10.1146/annurev-statistics-062713-085831>.
- Gneiting, T., and R. Ranjan, 2013: Combining predictive distributions. *Electronic Journal of Statistics*, **7**, 1747–1782.
- Gneiting, T., L. Stanberry, E. P. Gneiting, L. Held, and N. A. Johnson, 2008: Assessing probabilistic forecasts of multivariate quantities, with an application to ensemble predictions of surface winds. *TEST*, **17**.
- Goodfellow, I., Y. Bengio, and A. Courville, 2016: *Deep learning*. MIT press.
- Graziani, C., R. Rosner, J. M. Adams, and R. L. Machete, 2021: Probabilistic recalibration of forecasts. *International Journal of Forecasting*, **37** (1), 1–27, <https://doi.org/https://doi.org/10.1016/j.ijforecast.2019.04.019>, URL <https://www.sciencedirect.com/science/article/pii/S016920701930158X>.
- Grover, A., A. Kapoor, and E. Horvitz, 2015: A deep hybrid model for weather forecasting. *ACM SIGKDD International Conference on Knowledge Discovery and Data Mining*.
- Hirschberg, P. A., and Coauthors, 2011: A weather and climate enterprise strategic implementation plan for generating and communicating forecast uncertainty information. *Bulletin of the American Meteorological Society*, **92** (12), 1651–1666.
- Izmailov, P., P. Kirichenko, M. Finzi, and A. G. Wilson, 2020: Semi-supervised learning with normalizing flows. *International Conference on Machine Learning*, PMLR, 4615–4630.
- Jergensen, E., A. McGovern, R. Lagerquist, and T. Smith, 2020: Classifying convective storms using machine learning. *Weather and Forecasting*.
- Kingma, D. P., and P. Dhariwal, 2018: Glow: Generative flow with invertible 1×1 convolutions. *Advances in Neural Information Processing Systems*.
- Knutti, R., and J. Sedláček, 2013: Robustness and uncertainties in the new cmip5 climate model projections. *Nature Climate Change*, **3** (4), 369–373.
- Kobyzev, I., D. Prince, Simon. J., and M. A. Brubaker, 2019: Normalizing flows: An introduction and review of current methods. *IEEE Transactions on Pattern Analysis and Machine Intelligence*, 1–16.
- Kullback, S., and R. A. Leibler, 1951: On Information and Sufficiency. *The Annals of Mathematical Statistics*, **22** (1), 79 – 86, <https://doi.org/10.1214/aoms/117729694>, URL <https://doi.org/10.1214/aoms/117729694>.
- Leiva-Murillo, J. M., and A.-R. Antonio, 2007: Maximization of mutual information for supervised linear feature extraction. *IEEE Transactions on Neural Networks*, **18**.
- Lim, B., and Z. Stephen, 2021: Time-series forecasting with deep learning: a survey. *Philosophical Transactions of the Royal Society*.
- Mehrkanoon, S., 2019: Deep shared representation learning for weather elements forecasting. *Knowledge-Based Systems*.
- Nandar, A., 2009: Bayesian network probability model for weather prediction. *Current Trends in Information Technology*.
- Palmer, T., 2002: The economic value of ensemble forecasts as a tool for risk assessment: From days to decades. *Q.J.R. Meteorol. Soc.*, **128**.
- Petersik, P. J., and H. A. Dijkstra, 2020: Probabilistic forecasting of el niño using neural network models. *Geophysical Research Letters*.
- Qui, M., P. Zhao, K. Zhang, J. Huang, X. Shi, X. Wang, and W. Chu, 2017: A short-term rainfall prediction model using multi-task convolutional neural networks. *IEEE International Conference on Data Mining*.
- Roebber, P. J., M. R. Butt, S. J. Reinke, and T. J. Grafenauer, 2007: Real-time forecasting of snowfall using a neural network. *Weather and Forecasting*.
- Roulston, M. S., and L. A. Smith, 2002: Evaluating probabilistic forecasts using information theory. *Monthly Weather Review*, **130** (6), 1653–1660, [https://doi.org/10.1175/1520-0493\(2002\)130<1653:EPFUIT>2.0.CO;2](https://doi.org/10.1175/1520-0493(2002)130<1653:EPFUIT>2.0.CO;2), URL [https://doi.org/10.1175/1520-0493\(2002\)130<1653:EPFUIT>2.0.CO;2](https://doi.org/10.1175/1520-0493(2002)130<1653:EPFUIT>2.0.CO;2), [https://doi.org/10.1175/1520-0493\(2002\)130<1653:EPFUIT>2.0.CO;2](https://doi.org/10.1175/1520-0493(2002)130<1653:EPFUIT>2.0.CO;2).
- Salinas, D., V. Flunkert, J. Gasthaus, and T. Januschowski, 2020: Deepar:probabilistic forecasting with autoregressive recurrent networks. *International Journal of Forecasting*.
- Schaumann, P., R. Hess, M. Rempel, and V. Schmidt, 2021: A calibrated and consistent combination of probabilistic forecasts for the exceedance of several precipitation thresholds using neural networks. *Weather and Forecasting*.
- Shadvar, A., 2012: Dimension reduction by mutual information feature extraction. *International Journal of Computer Science & Information Technology*, **4**.
- Shi, X., and D.-Y. Yeung, 2018: Machine learning for spatiotemporal sequence forecasting: A survey. *ArXiv*, **abs/1808.06865**.
- Silverman, B., 2018: *Density Estimation for Statistics and Data Analysis*. CRC Press, URL <https://books.google.com/books?id=wIQPEAAQBAJ>.
- Sprenger, M., S. Schemm, R. Oechslein, and J. Jenkner, 2017: Nowcasting foehn wind events using the adaboost machine learning algorithm. *Weather and Forecasting*.
- Toth, Z., and R. Buizza, 2019: Weather forecasting: What sets the forecast skill horizon? *Sub-Seasonal to Seasonal Prediction*, Elsevier, 17–45.
- Van den Dool, H., P. S. Cpc, and H. Van Den Dool, 2007: *Empirical methods in short-term climate prediction*. Oxford University Press on Demand.
- Vossen, J., B. Feron, and A. a. Monti, 2018: Probabilistic forecasting of household electrical load using artificial neural networks. *IEEE Conference on Probabilistic Methods Applied to Power Systems*.
- Wang, J., and V. R. Kotamarthi, 2014: Downscaling with a nested regional climate model in near-surface fields over the contiguous united states. *Journal of Geophysical Research: Atmospheres*, **119** (14), 8778–8797.
- Yuan, H., G. Xiangong, S. L. Mullen, S. Sorooshian, J. Du, and H.-M. H. Juang, 2007: Calibration of probabilistic quantitative precipitation forecasts with an artificial neural network. *Weather and Forecasting*.

Zhu, Y., Z. Toth, R. Wobus, D. Richardson, and K. Mylne, 2002: The economic value of ensemble-based weather forecasts. *Bulletin of the American Meteorological Society*, **83**.

Ziegler, Z. M., and A. M. Rush, 2019: Latent normalizing flows for discrete sequences. *Proceedings of the 36th International Conference on Machine Learning, ICML*.

APPENDIX

A1. Modeling Winds via Normalizing Flows

The data at hand are often quite complex. As can be seen from Figure 1, the response itself has quite a complex form, taking the form of a doughnut shaped probability distribution. The inherent complexity of the data is only exacerbated by the packing of high dimensional information into a low dimensional form. Because of this, quite expressive models must be used to capture the detail in these distributions. In the context of modeling via normalizing flows, such data demand the use of flexible, non-naive architectures modeling ϕ , preferably in addition to expressive latent spaces.

Design of non-naive and expressive layers in the construction of normalizing flows is tricky given that invertibility must be guaranteed. The architectural component most heavily relied on in our modeling is what has been called the ‘‘coupling flow’’ in the literature. At the input to each coupling flow layer, an input $v \in \mathbb{R}^{p+m}$ is divided into two components $v^A \in \mathbb{R}^r$ and $v^B \in \mathbb{R}^{p+m-r}$. The coupling flow transforms the input by pushing v^A forwards by some invertible function h , and transforms v^B by the identity transform.

We define our coupling function $h : \mathbb{R}^r \rightarrow \mathbb{R}^r$ element-wise; let $\tilde{h} : \mathbb{R} \rightarrow \mathbb{R}$, $\tilde{h}_\theta(x) = ax + b + \frac{c}{1+(dx+h)}$, $\theta = [a, b, c, d, g]$, and finally $h(v) = (\tilde{h}_{\theta_1}(v_1), \dots, \tilde{h}_{\theta_r}(v_r))$. We model θ_i as the transformed output of a shallow neural network $\Theta_i : \mathbb{R}^{p+m-r} \rightarrow \mathbb{R}^5$, $\Theta_i(v^B) = \theta'_i$, where specifically, θ_i is formed from $\theta'_i = [a', b', c', d', g']$ in the method of (Ziegler and Rush 2019) to guarantee the invertibility of h :

$$a = a', \quad b = e^{b'}, \quad c = \frac{8\sqrt{3}}{9d} \tanh(c'), \quad d = e^{d'}, \quad g = g'.$$

This particular coupling function h is well-known in the literature, and has been noted in (Kobyzev et al. 2019) for its particular expressive power.

So far, no fancy architecture has been used to model Θ_i . As of now, we model

$$\Theta_i \in \left\{ f : \mathbb{R}^r \rightarrow \mathbb{R}^5 \mid f = R \circ A^{(l)} \circ \dots \circ R \circ A^{(1)} + L \right\},$$

i.e. we learn a fully connected network with linear residual connection, and ReLu activations. The residual connections are suggestion of (Kingma and Dhariwal 2018). We let l range between 3 and 10 in our experiments, and $l \approx 5$ is the general default setting. The choice of l does not appear to be terribly important as long as $l \geq 3$, which guarantees a flexible mapping.

The choice of which coordinates go into which component is a hyperparameter. As of now, it seems usually sufficient to have v^A be the coordinates corresponding to response and v^B be the coordinates corresponding to the predictors in one ‘‘coupling layer’’ and vice versa in a second coupling layer. These two make up the entire ϕ architecture. It is possible to stack further coupling flows on top of each other in the case that more model flexibility is required.

The choice of latent distribution, i.e. the choice of p_W , is an even more important hyperparameter. In practice, we have found it a useful addition to the complexity of the model to let p_W be the density of a normal mixture (Izmailov et al. 2020). As with all latent distributions, we treat the parameters ω as trainable, so the only choice to be made by the user is the number of mixture components. We have had success using anywhere between 1 and 20 mixture components, with more mixture components leading to more complex models. Stacking many coupling flows on top of each other may lead to numerical instabilities in the inversion of ϕ , so this can be quite useful. If more naive architectures are used to model ϕ , using 20 or more mixture components can be a saving grace.

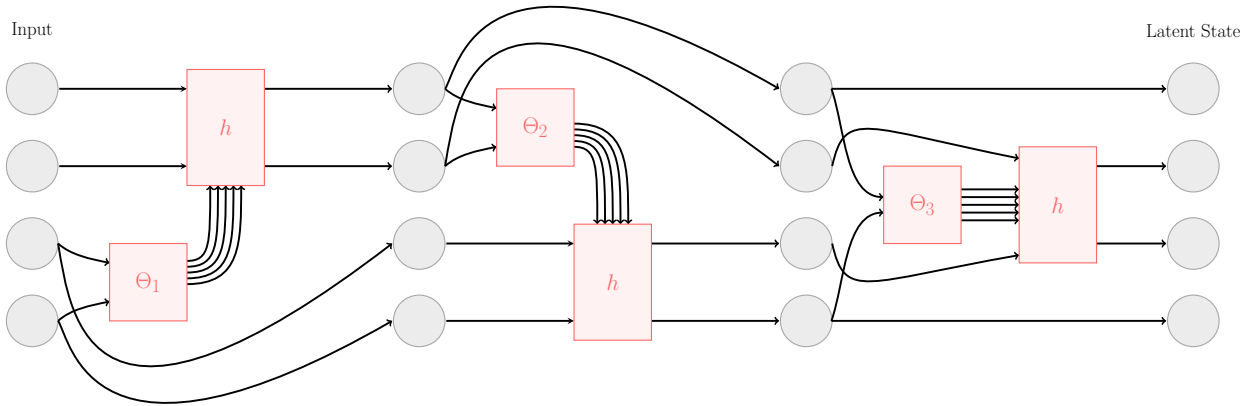


FIG. A1. A visualization of the normalizing flow architecture used.

Hyperparameter		Min. Value	Max. Value	In Experiments
Latent Distribution				
	Choice	Gaussian Mixture	Gaussian Mixture	Gaussian Mixture
	Mixture Components	3	20	5
	Train Latent Dist. Params.	True	True	True
Θ-Network				
	Θ-Net Depth	3	9	7
	Θ-Net ResNet	False	True	True
Core Training Params.				
	Training Iter.	200	4000	1200
	Batch Size	75	500	150
	Learning Rate	.01	.01	.01
	Optimizer	Adam	Adam	Adam
	β_1	.99	.99	.99
	β_2	.99	.99	.99
	Calibration Check Interval	50	200	100

TABLE A1. An overview of specific hyperparameter choices made.